Journal of Alloys and Compounds 498 (2010) 191–198

Contents lists available at ScienceDirect

Journal of Alloys and Compounds

journal homepage: www.elsevier.com/locate/jallcom

Temperature dependent elastic coefficients of Mg_2X (X = Si, Ge, Sn, Pb) compounds from first-principles calculations

S. Ganeshan*, S.L. Shang, Y. Wang, Z.-K. Liu

Department of Materials Science and Engineering, The Pennsylvania State University, University Park, PA 16802, United States

ARTICLE INFO

Article history:
Received 26 January 2010
Received in revised form 16 March 2010
Accepted 17 March 2010
Available online 23 March 2010

Keywords:
Metals and alloys
Elasticity
Computer simulations

ABSTRACT

Influence of temperature on the elastic properties of Mg_2X (X = Si, Ge, Sn, and Pb) compounds, has been studied using first-principles calculations, within the generalized gradient approximation, and compared with the available experimental data in the literature. Elastic stiffness coefficients calculated with respect to volume ($c_{ij}(V)$) have been correlated to the equilibrium volume as a function of temperature $V(T)$ from phonon calculations to obtain temperature dependence of elastic stiffness coefficients $c_{ij}(T)$. A good agreement between the thus predicted elastic constants and experimental data has been achieved. The general trend in the bulk modulus (B), shear modulus (G) and Young's modulus (E) seen for the compounds is $Mg_2Ge > Mg_2Si > Mg_2Sn > Mg_2Pb$. Elastic anisotropy, fracture toughness and stiffness of the compounds have been analyzed as a function of temperature based on their anisotropic ratio ($2c_{44}/(c_{11}-c_{12})$), product of bulk modulus and volume ($B \times V^{1/3}$), and Young's modulus. The results obtained herein provide a better understanding of the elastic behavior of antifluorite compounds as a function of temperature. The methodology used in this work acts as a benchmark for future first-principles work that involves calculating elastic constants as a function of temperature.

1. Introduction

The antifluorite structured Mg_2X compounds, where X = Si, Ge, Sn, and Pb, have always been of keen interest in several areas of research. Some recent investigations include [1–6]. Except for Mg_2Pb, which is more prominent as a semi-metal [7,8], the other compounds mentioned above are semi-conductors [1,9,10]. Owing to their intriguing properties like exceptionally good thermoelectric characteristics [2,5,6,11], low density, low coefficient of thermal expansion, high hardness and high elastic modulus, the range of applications where Mg_2X compounds can be employed is constantly increasing [12–14]. Recently, Mg_2X compounds have also been shown to be better replacers for Mg-RE (rare earth) compounds because of their above mentioned properties and the fact that they are relatively cheaper [12].

Although a reasonable amount of information about the room temperature behaviors of these compounds does exist [8,12,15], there is a dearth of data in terms of the temperature dependency of their properties. To be able to use these compounds for applications at elevated temperatures, knowledge of their basic properties at the corresponding temperatures is imperative. Elastic constants are one such material property that builds a foundation for a better understanding of various other properties, be it mechanical, physical or even electronic [16–19]. Lately, elastic constants have been correlated to properties like hardness [19,20], fracture toughness [21], stiffness, ductility and bond characteristics [22–24]. Elastic constants are also vital in considering defects in solids [25] such as vacancies [26], interstitials, substitutional impurities, dislocations, twin boundaries [27] and grain boundary energies [28].

While experimental determination of elastic constants of compounds at temperatures above room temperature has always been challenging, no theoretical calculations have either been reported in the literature for these compounds. We have recently started research activities in this area [29–31]. In the current work, we present elastic stiffness coefficients, c_{ij}, bulk modulus, B, shear modulus, G, Young's modulus, E, Poisson's ratio, υ, and anisotropic ratio, A of the II–IV group compounds (Mg_2Si, Mg_2Ge, Mg_2Sn and Mg_2Pb), from first-principles calculations. It aims to provide not only useful data for these compounds but also a benchmark methodology for obtaining elastic stiffness coefficients as a function of temperature in general.

2. Methodology

In the present work, first-principles calculations based on density functional theory [32] is performed. The generalized gradient approximation (GGA) of Perdew–Burke–Ernzerhof (PBE) [33] as implemented in the Vienna Ab-initio Simulation Package (VASP) [34,35] has been employed. The ion–electron interaction is described using the projector augmented wave method (PAW) [36]. A primitive

* Corresponding author at: Department of Materials Science and Engineering, 304 Steidle Building, University Park, PA 16802, United States.
E-mail address: sxg319@psu.edu (S. Ganeshan).

0925-8388/$ – see front matter © 2010 Elsevier B.V. All rights reserved.
doi:10.1016/j.jallcom.2010.03.153

unit cell containing 1 formula unit has been used for calculation of total energy as well as elastic stiffness coefficients. Since all the four compounds in the current study possess an FCC-antifluorite structure, a Monkhorst-Pack [37] k-point set of $15 \times 15 \times 15$ with an energy cut-off of 350 eV is used after having tested for convergence. The atomic arrangements are relaxed using the Methfessel–Paxton [38] technique for the reciprocal-space integration, following which accurate stresses of the relaxed structures are obtained using the tetrahedron method with Blöchl corrections [39].

2.1. Elastic coefficients

Herein, elastic stiffness coefficients for each of the (Mg_2X) compounds are calculated at 8 different volumes that have been generated around the equilibrium volume, such that the maximum total strain is related to the lattice constant near the melting point of each of the structures. The effective stress–strain method [22,40,41] has been used to calculate the elastic stiffness coefficients at each volume. As per this method, a set of strains, $\varepsilon = (\varepsilon_1, \varepsilon_2, \varepsilon_3, \varepsilon_4, \varepsilon_5, \varepsilon_6)$, where $\varepsilon_1, \varepsilon_2, \varepsilon_3$ refer to normal strains and ε_4, ε_5, ε_6 to shear strains, is imposed on the fully relaxed crystal structure of the compound. Let (Q) and ($\tilde{Q}$) represent the crystal lattice vectors before and after the application of strains such that,

$$\tilde{Q} = Q \begin{pmatrix} 1+\varepsilon_1 & \varepsilon_6/2 & \varepsilon_5/2 \\ \varepsilon_6/2 & 1+\varepsilon_2 & \varepsilon_4/2 \\ \varepsilon_5/2 & \varepsilon_4/2 & 1+\varepsilon_3 \end{pmatrix} \tag{1}$$

Thereafter for each of the strains applied corresponding stresses, $\sigma = (\sigma_1, \sigma_2, \sigma_3, \sigma_4, \sigma_5, \sigma_6)$, are obtained from first-principles total energy calculations. From the n set of strains (ε) and the resulting stresses (σ), elastic stiffness coefficients (c_{ij}'s) are then calculated based on Hooke's law, as shown below:

$$\begin{pmatrix} c_{11} & c_{12} & c_{13} & c_{14} & c_{15} & c_{16} \\ c_{21} & c_{22} & c_{23} & c_{24} & c_{25} & c_{26} \\ c_{31} & c_{33} & c_{33} & c_{34} & c_{35} & c_{36} \\ c_{41} & c_{42} & c_{43} & c_{44} & c_{45} & c_{46} \\ c_{51} & c_{52} & c_{53} & c_{54} & c_{55} & c_{56} \\ c_{61} & c_{62} & c_{63} & c_{64} & c_{65} & c_{66} \end{pmatrix} = \begin{pmatrix} \varepsilon_{1,1} & \dots & \varepsilon_{1,n} \\ \varepsilon_{2,1} & \dots & \varepsilon_{2,n} \\ \varepsilon_{3,1} & \dots & \varepsilon_{3,n} \\ \varepsilon_{4,1} & \dots & \varepsilon_{4,n} \\ \varepsilon_{5,1} & \dots & \varepsilon_{5,n} \\ \varepsilon_{6,1} & \dots & \varepsilon_{6,n} \end{pmatrix}^{-1} \begin{pmatrix} \sigma_{1,1} & \dots & \sigma_{1,n} \\ \sigma_{2,1} & \dots & \sigma_{2,n} \\ \sigma_{3,1} & \dots & \sigma_{3,n} \\ \sigma_{4,1} & \dots & \sigma_{4,n} \\ \sigma_{5,1} & \dots & \sigma_{5,n} \\ \sigma_{6,1} & \dots & \sigma_{6,n} \end{pmatrix} \tag{2}$$

In the present study six linearly independent set of strains are applied such that

$$\begin{pmatrix} \varepsilon_{1,1} & \dots & \varepsilon_{1,6} \\ \varepsilon_{2,1} & \dots & \varepsilon_{2,6} \\ \varepsilon_{3,1} & \dots & \varepsilon_{3,6} \\ \varepsilon_{4,1} & \dots & \varepsilon_{4,6} \\ \varepsilon_{5,1} & \dots & \varepsilon_{5,6} \\ \varepsilon_{6,1} & \dots & \varepsilon_{6,6} \end{pmatrix} = \begin{pmatrix} x & 0 & 0 & 0 & 0 & 0 \\ 0 & x & 0 & 0 & 0 & 0 \\ 0 & 0 & x & 0 & 0 & 0 \\ 0 & 0 & 0 & x & 0 & 0 \\ 0 & 0 & 0 & 0 & x & 0 \\ 0 & 0 & 0 & 0 & 0 & x \end{pmatrix}$$

with $x = \pm 0.01$ Å.

For the FCC-antifluorite structure studied in the present work, the number of independent components of elastic stiffness tensor decreases to 3, i.e., c_{11}, c_{12}, and c_{44}.

Eq. (2) can thereby be written in a simplified form as follows:

$$\begin{pmatrix} c_{11} & c_{12} & c_{12} & 0 & 0 & 0 \\ c_{12} & c_{11} & c_{12} & 0 & 0 & 0 \\ c_{12} & c_{12} & c_{11} & 0 & 0 & 0 \\ 0 & 0 & 0 & c_{44} & 0 & 0 \\ 0 & 0 & 0 & 0 & c_{44} & 0 \\ 0 & 0 & 0 & 0 & 0 & c_{44} \end{pmatrix} = \begin{pmatrix} \varepsilon_{1,1} & \dots & \varepsilon_{1,6} \\ \varepsilon_{2,1} & \dots & \varepsilon_{2,6} \\ \varepsilon_{3,1} & \dots & \varepsilon_{3,6} \\ \varepsilon_{4,1} & \dots & \varepsilon_{4,6} \\ \varepsilon_{5,1} & \dots & \varepsilon_{5,6} \\ \varepsilon_{6,1} & \dots & \varepsilon_{6,6} \end{pmatrix}^{-1} \begin{pmatrix} \sigma_{1,1} & \dots & \sigma_{1,6} \\ \sigma_{2,1} & \dots & \sigma_{2,6} \\ \sigma_{3,1} & \dots & \sigma_{3,6} \\ \sigma_{4,1} & \dots & \sigma_{4,6} \\ \sigma_{5,1} & \dots & \sigma_{5,6} \\ \sigma_{6,1} & \dots & \sigma_{6,6} \end{pmatrix} \tag{3}$$

The bulk (B), shear (G), and Young's (E) moduli and Poisson's ratio (υ) for the cubic compounds in the current work are computed using Hill's [42] approximation as shown below:

$$B_H = B_V = B_R = \frac{c_{11} + 2c_{12}}{3} \tag{4}$$

$$G_H = \frac{G_V + G_R}{2}, \quad \text{where } G_V = \frac{c_{11} - c_{12} + 3c_{44}}{5} \text{ and } G_R = \frac{5(c_{11} - c_{12})c_{44}}{4c_{44} + 3(c_{11} - c_{12})} \tag{5}$$

$$E_H = \frac{9B_H G_H}{3B_H + G_H} \tag{6}$$

$$\upsilon = \frac{3B_H - 2G_H}{2(3B_H + G_H)} \tag{7}$$

where subscripts V and R refer to Voigt [43] and Reuss [44] approximations.

2.2. Phonon dispersion curves and phonon density of states

Phonon calculations are carried out using the supercell method as implemented in the ATAT code [45]. The supercell method involves calculating the forces that result from perturbing atoms from their equilibrium positions. Phonon calculations via the supercell method begin with generating supercells from the fully relaxed primitive cells for each of the systems under study. The present study consists of quasiharmonic calculations with 8 different volumes. For each of the volumes, different supercells are generated with perturbations corresponding to the atomic positions and their energies and inter-atomic forces are calculated with no relaxation of their degrees of freedom [46–48]. Displacements of 0.15 Å are applied to the ions. Supercells consisting of 81 atoms for Mg_2Si and Mg_2Ge and 96 atoms for Mg_2Sn and Mg_2Pb are created. The size of the supercell has been chosen such that the force constant decreases to a negligibly small value from the equilibrium position of the perturbed atom to the boundary of the supercell. A Monkhorst-Pack [37] k-point mesh of $4 \times 4 \times 4$ is applied along with a cut-off energy of 350 eV. Force constants are obtained using the *fitfc* code within the ATAT package [45]. Herein a cut-off range of 6 Å is used. Finally phonon frequencies are calculated within the assigned range of force constants.

By using the resultant phonon density of states (DOS), the vibrational free energy (F_{vib}) of the system in units of eV/atom is obtained using the following equation [49]:

$$F_{vib}(T) = k_B T \int_0^\infty d\nu \ \ln \left[2 \sin h \left(\frac{h\nu}{2k_B T} \right) \right] \cdot g(\nu) \tag{8}$$

where ν is the phonon frequency and $g(\nu)$ corresponds to the phonon DOS. From this vibrational free energy, bulk modulus as a function of temperature ($B(T)$) and thereby temperature dependent heat capacity, $C_p(T)$, are obtained as shown in Eqs. (9) and (10):

$$B(T) = V_T \left(\frac{\partial^2 F_{vib}}{\partial V^2} \right)_T \tag{9}$$

$$C_p(T) = C_V(T) + \beta^2 B_T T V_T \tag{10}$$

where C_v and C_P are heat capacity at constant volume and constant pressure, respectively, estimated by $C_V = T(\partial s/\partial T)_V$. B_T, T, and V_T are the bulk modulus, temperature and volume. β is the volume thermal expansion coefficient which is 3 times the linear coefficient of expansion given by $\alpha_T = (1/3\nu_0 T)(\partial \nu_0 T/\partial T)_p$, where V_{0T} is the equilibrium volume at the temperature of interest.

2.3. Transitive correlation method for temperature dependent c_{ij}'s

The methodology incorporated in this study to calculate elastic stiffness coefficients as a function of temperature is as follows [29,30]. First, elastic stiffness coefficients at different volumes, $c_{ij}(V)$, are calculated at 0 K from first-principles based on the effective stress–strain method [40,41] along with phonon calculations at different volumes. From these quasiharmonic phonon calculations we obtain vibrational free energy, specific heat, bulk modulus, and volume under the pressure of interest (external pressure of 0 kB has been used in the present work). At this point, it is assumed that the volumes for which elastic stiffness coefficients have been calculated at 0 K correspond to the volumes as a function of temperature obtained from the first-principles quasiharmonic calculations. Hence, under the framework of quasiharmonic approach, we obtain temperature dependent, $c_{ij}(T)$, based on the predicted $c_{ij}(V)$ and $V(T)$ mentioned above. The polynomial fitting parameters used in obtaining $c_{ij}(T)$ is shown in Table 1.

Since calculated elastic stiffness coefficients obtained herein are under isothermal conditions and the experimental measurements are isentropic, a correction term (see Eq. (11)) has been added to our results as per [29,30,50] for c_{11} and c_{12}. Incorporating the correction terms resulted in an increase in the elastic stiffness coefficients by a maximum of ~5.7 GPa for Mg_2Si and ~5.85 GPa for Mg_2Ge, ~3.8 GPa for Mg_2Sn and ~3 GPa for Mg_2Pb at their respective melting temperatures. It is understood from the results in the present work that the correction term becomes more significant at higher temperatures (see Fig. 1). The isentropic correction term

Table 1
Polynomial fitting parameters that have been used in this work to calculate c_{ij} as a function of temperature (T); ($a + bT + cT^2$).

Compound	c_{ij} (GPa)	a (GPa)	b (GPa/K)	c (GPa/K^2)
Mg_2Pb	c_{11}	54.494	−0.0072	-5×10^{-6}
	c_{12}	22.570	−0.0025	-2×10^{-6}
	c_{44}	23.961	−0.0033	-2×10^{-6}
Mg_2Sn	c_{11}	70.583	−0.0063	-3×10^{-6}
	c_{12}	25.355	−0.0024	-2×10^{-6}
	c_{44}	30.317	−0.0030	-1×10^{-6}
Mg_2Ge	c_{11}	117.48	−0.0076	-3×10^{-6}
	c_{12}	24.223	−0.0028	-1×10^{-6}
	c_{44}	46.018	−0.0044	-2×10^{-6}
Mg_2Si	c_{11}	115.13	−0.0072	-3×10^{-6}
	c_{12}	22.112	−0.0024	-1×10^{-6}
	c_{44}	44.707	−0.0043	-2×10^{-6}

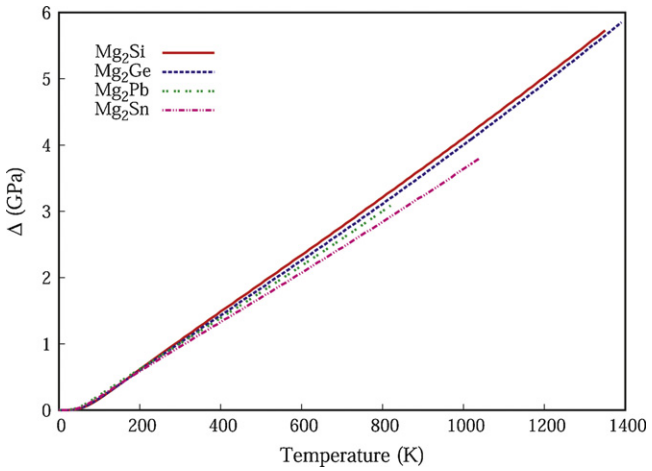

Fig. 1. Isentropic correction term (△) as a function of temperature calculated in present work.

for c_{11} and c_{12} is given by [30]:

$$\Delta = \frac{T * V_T * (\beta_T * B_T)^2}{C_v} \quad (11)$$

where T is temperature, V_T, α_T, B_T and C_v correspond to volume, coefficient of thermal expansion, bulk modulus, and heat capacity obtained from phonon calculations. Figs. 2, 4 and 5 show volume, coefficient of thermal expansion, heat capacity and bulk modulus for each of the compounds, obtained from phonon calculations, as a function of temperature.

3. Results and discussion

This section is divided into three parts. In Section 3.1, we provide comparative results between calculated data for phonon dispersion curves and heat capacities from the current work and available experimental data in the literature to verify the quality of our phonon calculations. In Section 3.2, a proof that the transitive correlation methodology mentioned in Section 2.3 works well is shown by comparing bulk modulus with data from direct phonon calculations. Finally in Section 3.3, we present results for elastic stiffness coefficients with respect to temperature as calculated in the current work along with a detailed analysis of the results and a comparison with available experimental data in the literature.

3.1. Validity of phonon calculations

Experimental measurements for phonon dispersion curves are available for Mg_2Pb [51] and Mg_2Sn [52]. Measurements for both compounds were carried out using neutron inelastic scattering. The phonon dispersion curves for the four compounds are shown in Fig. 3. As seen in Fig. 3 the present calculations agree well with the available measurements, especially for the acoustic branches. These results indicate that our phonon calculations are of high quality.

Fig. 4 shows calculated heat capacity, C_P, data along with available experimental data [13,53–55] for the compounds studied herein. Calculated data is plotted from 0 K to the approximate melting point of the compounds [56]. Experimental measurements for heat capacity data were available from 15 to 300 K for Mg_2Si [54] and from 5 to 300 K for the other three compounds [13,53,55]. Measurements for these compounds were made by the same group. The authors indicate a considerable amount of scatter at low temperatures especially below 15 K. As apparent from Fig. 4, there is an excellent agreement between our calculated results and measured data.

3.2. Applying the transitive correlation to bulk modulus

In order to ensure that the correlation made in this study, i.e., $c_{ij}(V) \overset{V(T)}{\Leftrightarrow} C_{ij}(T)$ is reasonable, we present firstly results for bulk modulus of these compounds. The reason for choosing bulk modulus is because temperature dependent bulk modulus can be obtained directly from both quasiharmonic phonon calculations and $c_{ij}(T)$. Fig. 5 shows isothermal B vs. T curves from both approaches. Since the bulk modulus obtained from quasiharmonic phonon calculations is not isentropic, we have not applied correction terms for the bulk modulus obtained from $c_{ij}(T)$ in this present comparison. In general, from Fig. 5 it is clear that a good agreement lies between the results obtained from quasiharmonic approach as well as from the transitive correlation approach. Specifically for Mg_2Pb and Mg_2Si the comparisons appear very promising. While for Mg_2Ge and Mg_2Sn, an overestimation of ~2 GPa arises above room temperature, the difference between the curves, with respect to the quasiharmonic approach lies within 4% for all the compounds. Thus, it can be concluded that the data obtained for bulk modulus from the transitive correlation is worthy for further consideration. With this in mind, we present in Section 3.3, results obtained for elastic stiffness coefficients as a function of temperature.

3.3. Elastic stiffness coefficients c_{ij}'s

The elastic stiffness coefficients and the corresponding bulk modulus, shear modulus, Young's modulus, Poisson's ratio, and anisotropy ratio of Mg_2Si, Mg_2Ge, Mg_2Sn, and Mg_2Pb have been calculated herein as per the procedure mentioned in Section 2.3. Fig. 6 shows calculated elastic stiffness coefficients as a function of temperature for all the four compounds considered herein along with the available experimental data. Experimental elastic constants were available for Mg_2Si measured by longitudinal and transverse

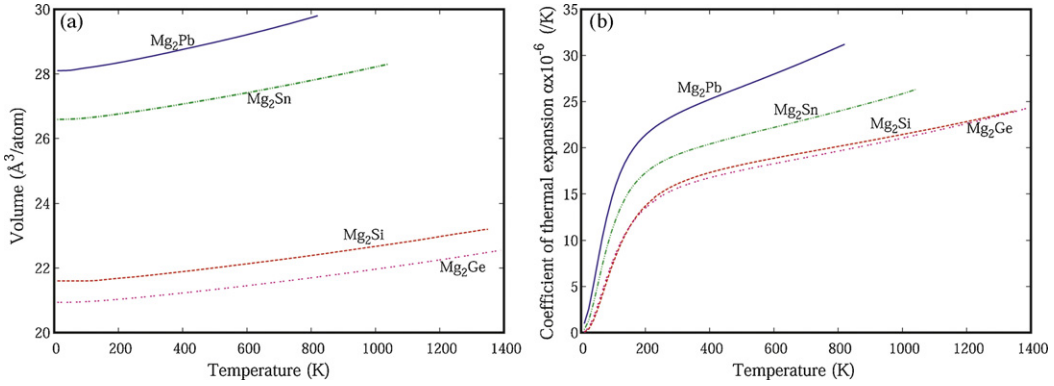

Fig. 2. Calculated (a) volume and (b) coefficient of thermal expansion as a function of temperature.

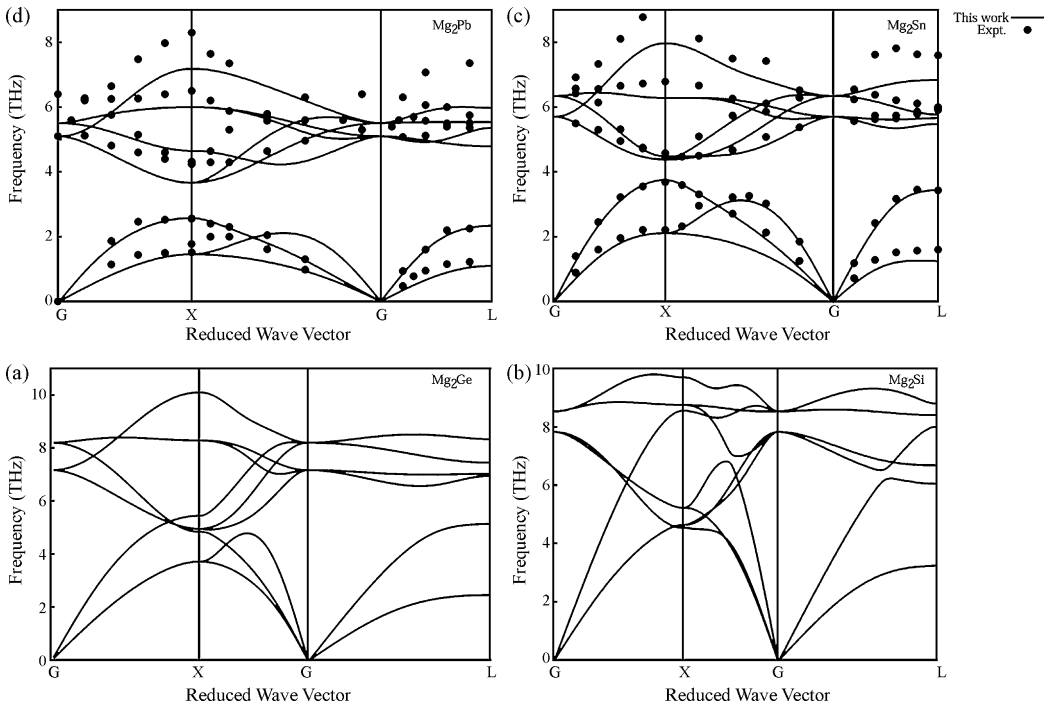

Fig. 3. Calculated phonon dispersion curves along with experimental data: (a) Mg_2Ge, (b) Mg_2Si, (c) Mg_2Pb [51] and (d) Mg_2Sn [52].

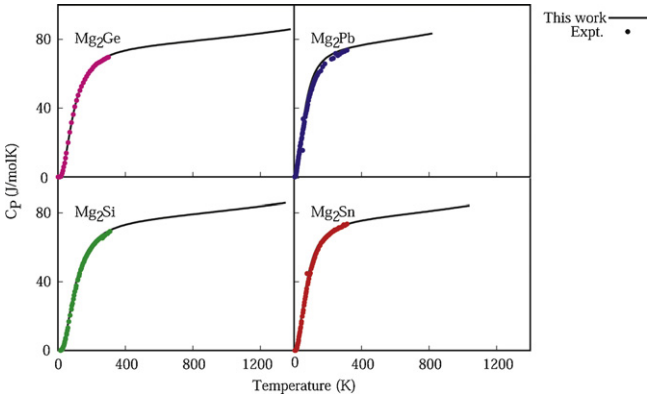

Fig. 4. Calculated and experimental [13,53–55] heat capacity of the Mg_2X compounds studied herein.

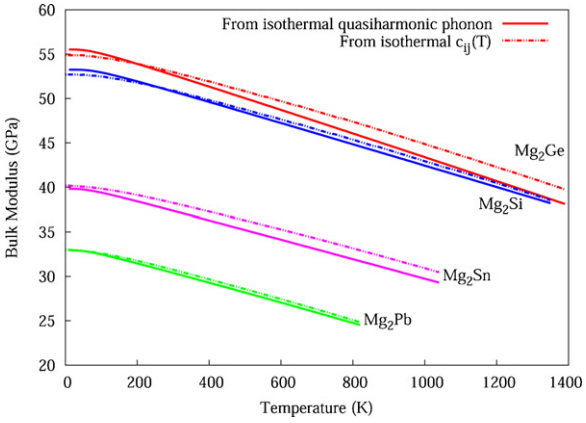

Fig. 5. A comparison between isothermal bulk modulus obtained directly from quasiharmonic approach through phonon calculations and from isothermal $c_{ij}(T)$ (i.e., without the addition of correction terms).

sound velocities from 80 to 300 K [57]. For Mg_2Ge [58] and Mg_2Sn [59] elastic constants were extrapolated by least square method from sound velocities measured by resonance technique from 80 to 300 K. In the case of Mg_2Pb [51] measurements for elastic constants were available only at room temperature. There is a very good agreement between calculated and experimental data for Mg_2Si and Mg_2Ge as seen in Fig. 6. However, due to the high level of uncertainty in the experimental data in the case of Mg_2Sn and the lack of measurements for Mg_2Pb, a reasonable comparison could not be made for these two compounds.

From the calculated results for the elastic stiffness coefficients, the influence of temperature on each of the c_{ij}'s can be observed. Of all the c_{ij}'s (i.e., c_{11}, c_{12} and c_{44}), c_{12} shows the maximum change up to the melting point for Mg_2Si, Mg_2Ge and Mg_2Sn. For instance, c_{11} and c_{44} of Mg_2Si decreases by ~15% and ~23%, whereas c_{12} decreases by ~ 33% from 0 K to the melting point. Similarly, for Mg_2Ge, c_{11} and c_{44} decrease only by ~16% and ~24%, but c_{12} decreases by almost 34%. Even in the case of Mg_2Sn the maximum influence of temperature is seen for c_{12}. In the case of Mg_2Pb, however, all the three elastic stiffness coefficients decrease uniformly by ~18%. The percentage decreases mentioned here have been rounded off to the nearest whole number. From Fig. 6, it can also be noted that the maximum elastic stiffness coefficients near the melting point pertains to c_{11} of Mg_2Ge (~101 GPa), and the minimum pertains to c_{12} of Mg_2Si (~16.4 GPa). It should be emphasized here that values for elastic stiffness coefficients for Mg_2Si and Mg_2Ge are very close to each other due to a high similarity in their structures.

On comparing the elastic stiffness coefficients for the four compounds, it is seen as in Fig. 7 that c_{11} and c_{44} show a similar trend, while c_{12} shows a different trend. In the case of c_{11} and c_{44}, the trend followed is $Mg_2Ge > Mg_2Si > Mg_2Sn > Mg_2Pb$, with Mg_2Si and Mg_2Ge being very close to each other in their elastic stiffness coefficients, whereas for c_{12} the trend seen is different. In the case of c_{12} Mg_2Sn has the highest value followed by Mg_2Ge, Mg_2Pb and Mg_2Si at their corresponding melting temperatures. However the trend seen in B, E, and G of these compounds is similar to those of c_{11} and c_{44}. The reason behind this difference in the trend of c_{12}

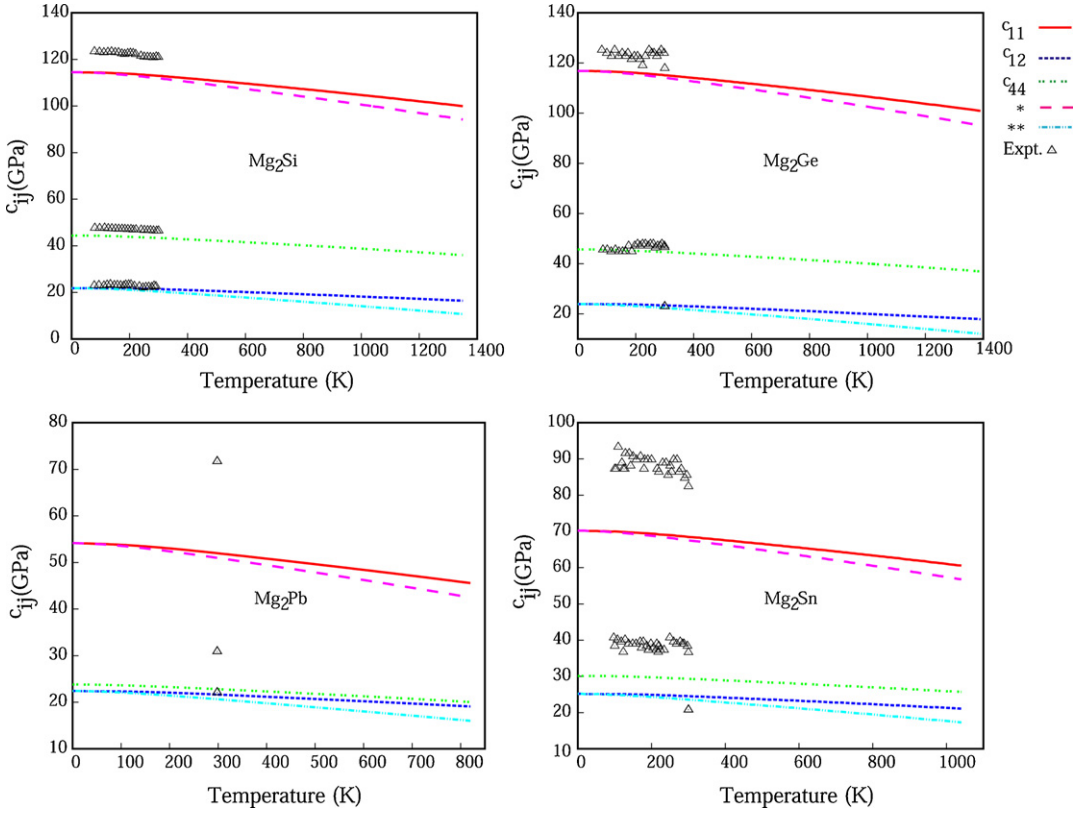

Fig. 6. Calculated isentropic c_{ij} as a function of temperature along with available experimental data [51,57–59] (* and ** refer to isothermal c_{11} and c_{12}, i.e., without the addition of correction term △).

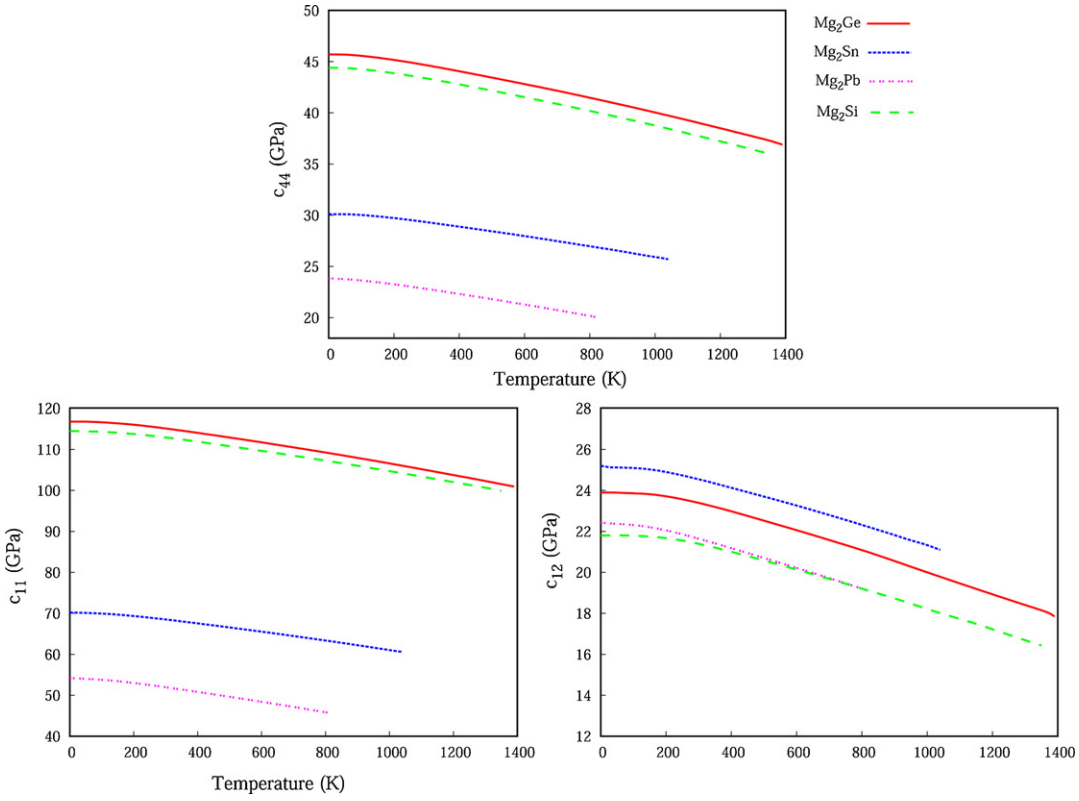

Fig. 7. Trends seen in the c_{ij} of each of the compounds as a function of temperature.

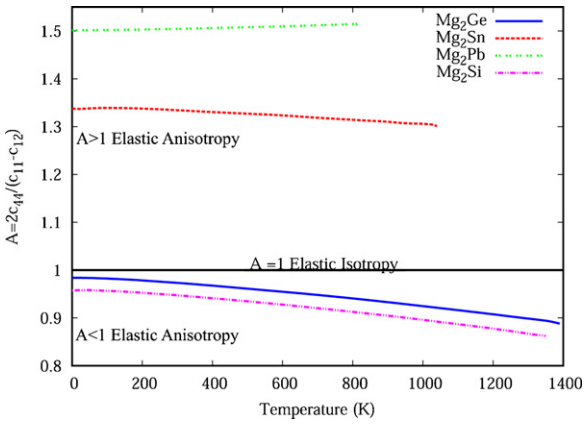

Fig. 8. Elastic anisotropy as a function of temperature for the compounds studied herein.

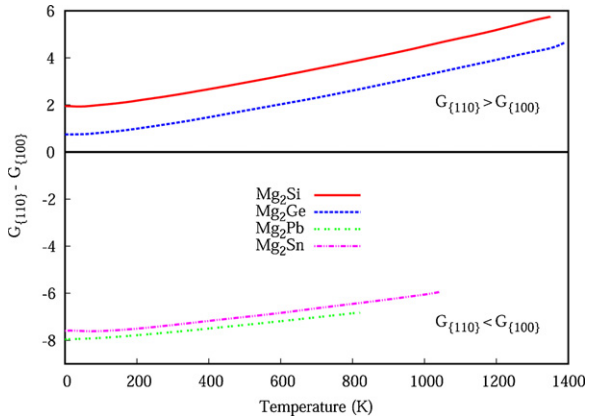

Fig. 9. Relative shear modulus as a function of temperature for the compounds considered in this work.

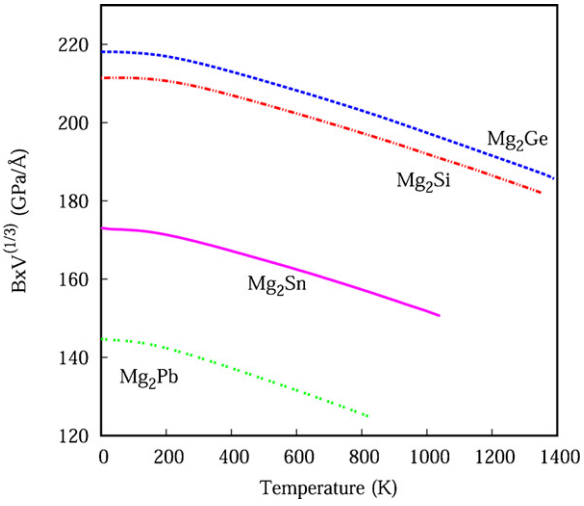

Fig. 10. Fracture strength of the compounds depicted by product of bulk modulus and volume as a function of temperature.

could be attributed to its lack of phonon physicality as mentioned by Ledbetter [60].

Based on the results obtained for the elastic stiffness coefficients the anisotropic ratio as a function of temperature for all the four compounds can be calculated using the following equation [16]:

$$A = \frac{2c_{44}}{c_{11} - c_{12}} \tag{12}$$

It is known that elastic anisotropy correlates to dielectric breakdown and resistance to micro-crack of a given material [61,62]. A large anisotropy tends to enhance cross-slip [63]. In Eq. (12), if $A = 1$ the material is considered to be completely isotropic, while the further the value of A from 1, the more anisotropic it is [16]. It has also been proposed that large values of A can give rise to the driving force (tangential force) acting on screw dislocations to promote cross-slip pinning process [64]. From Fig. 8 it is seen that none of the compounds considered in this study are completely elastically isotropic. All of them possess an anisotropy ratio either greater or less than 1. However, Mg_2Si and Mg_2Ge begin with values of A being very close to 1 at 0 K when compared to those of Mg_2Pb and Mg_2Sn. While the rate of change in the anisotropic ratio is moderate for all the compounds, Mg_2Pb shows the least amount of change in its anisotropic ratio. The value of A for Mg_2Pb begins with 1.50 at 0 K and ends at 1.51 near its melting point. Mg_2Si and Mg_2Ge compared to the other two compounds show greater changes in their anisotropic ratios. The value of A for Mg_2Si begins at 0.96 and ends at 0.86 showing an approximate decrease of 10% in its value. In the case of Mg_2Ge, the change in the anisotropic ratio is about 11%. Both Mg_2Ge and Mg_2Si become more elastically anisotropic with increasing temperature whereas Mg_2Sn becomes less anisotropic. Based on [61,62], it can be concluded that with the increase in temperature Mg_2Si and Mg_2Ge become less resistant to micro-cracks and the possibility of dielectric break down increases, while Mg_2Sn gains more resistance to the same. On an average, however, the anisotropic ratio for Mg_2Si and Mg_2Ge is still closer to 1 than the anisotropic ratio of Mg_2Sn. In the case of Mg_2Pb, the influence of temperature appears negligible on its anisotropy thereby causing its resistance to micro-cracks and dielectric breakdown to remain almost uniform.

Another important elastic property is the shear modulus that correlates to a material's resistance to shear and plastic deformation [27]. The shear moduli for the {1 0 0} plane along the [0 1 0] direction and for the {1 1 0} plane along the [1 $\bar{1}$ 0] direction are c_{44} and $(c_{11}-c_{12})/2$, represented by $G_{\{100\}}$ and $G_{\{110\}}$ [65]. Fig. 9 shows the difference in the corresponding single crystal shear moduli (i.e., $G_{\{110\}}-G_{\{100\}}$) for the compounds considered in this study. It is seen that for Mg_2Sn and Mg_2Pb, $G_{\{100\}}$ is always greater than $G_{\{110\}}$ at any temperature. This means that these compounds have a greater resistance to shear along the {1 0 0} plane than along the {1 1 0} plane [65]. For Mg_2Si and Mg_2Ge, as seen in Fig. 9, $G_{\{110\}}$ is always higher than $G_{\{100\}}$ indicating that it is easier to shear the materials along the {1 0 0} plane than the {1 1 0} plane [65].

On the relations between elastic moduli and plastic properties Pugh [18] suggested that the fracture stress (τ) of a material can be approximately correlated to $B \times a$, where B is the bulk modulus and a the lattice constant. Extending this relation to $BV^{1/3}$, with V being the volume of the unit cell as for a cubic system $a^3 = V$, we have attempted to study the fracture toughness behavior of these materials as a function of temperature. Though this is not an accurate comparison, a basic understanding of the strength of these materials can be obtained. Fig. 10 shows the value of $B \times V^{1/3}$ as a function of temperature for the compounds in this study. All the four compounds show a general decrease in their $B \times V^{1/3}$ value. It can be then concluded that the degree to which the bulk modulus of the compounds decrease with temperature is greater than the degree to which there is a volume increase as a function of temperature. Among the four compounds, Mg_2Ge has the highest value of ~185.6 GPa/Å, and Mg_2Pb has the lowest value of ~124.9 GPa/Å^3 at their respective melting temperatures. From the curves shown in Fig. 10, based on Pugh's [18] relation that $\tau \propto B \times V^{1/3}$, we can approximate that the least fracture strength as a function of temperature is shown by Mg_2Pb. Mg_2Sn has a higher fracture strength com-

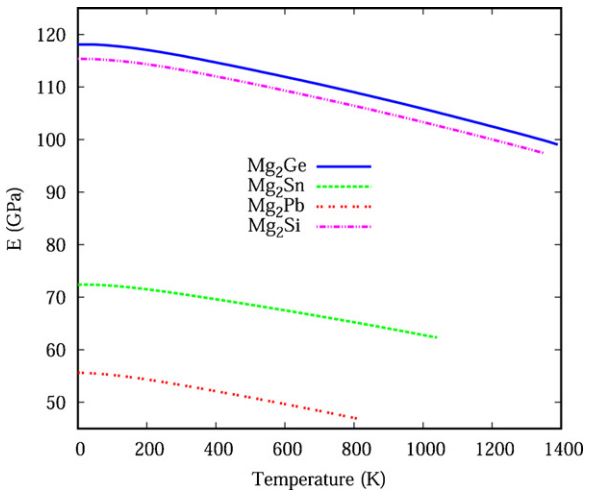

Fig. 11. Young's modulus (E) as a function of temperature.

pared to Mg_2Pb but has its $B \times V^{1/3}$ value lower than Mg_2Si and Mg_2Ge.

The stiffnesses of these compounds can be estimated based on their Young's modulus (E). The larger the value of E, the stiffer the material [65]. Change in E as a function of temperature for each of the compounds considered in this work is shown in Fig. 11. In agreement with the general trend, the Young's modulus decreases with temperature, indicating that the compounds become less stiff as the temperature increases. The maximum E at the melting temperature pertains to that of Mg_2Ge (~99.0 GPa), followed by Mg_2Si (~97.4 GPa), Mg_2Sn (~62.3 GPa) and finally Mg_2Pb (~46.7 GPa).

Apart from the above mentioned correlations, there are several other properties like machinability, ductility [66], bond characteristics, load deflection, etc. that can be understood for these materials based on their elastic stiffness coefficients. Some of these properties for the Mg_2X compounds have been studied at 0 K in our previous work [22].

4. Summary

First-principles calculations of elastic constants as a function of temperature have been performed for Mg_2X (X = Si, Ge, Sn, Pb) compounds. A good agreement between calculated and available experimental data in the literature is shown. The accuracy of the current first-principles calculations has been validated by comparing with experimental phonon dispersions and heat capacities as a function of temperature for all the compounds. The transitive correlation methodology employed here in calculating elastic stiffness coefficients as a function of temperature has been corroborated by presenting similar values for bulk modulus as obtained from the quasiphonon calculations. The elastic stiffness coefficients of the compounds decrease in the sequence of $Mg_2Ge > Mg_2Si > Mg_2Sn > Mg_2Pb$ for c_{11} and c_{44}, but in the sequence of $Mg_2Sn > Mg_2Ge > Mg_2Pb > Mg_2Si$, at their corresponding melting points, for c_{12}. All the compounds exhibit elastic anisotropy as a function of temperature. The value of the anisotropic ratio moves further away from 1 for Mg_2Si and Mg_2Ge; approaches 1 in the case of Mg_2Sn and remains almost constant for Mg_2Pb. Mg_2Sn and Mg_2Pb show greater resistance to shear along the {1 0 0} plane while Mg_2Si and Mg_2Ge show greater resistance to shear along the {1 1 0} plane. The fracture strength and stiffness of the compounds decrease with increase in temperature. The data obtained in this work not only provides the fundamental understanding of the elastic behavior of the antifluorite materials considered herein, but also acts as a benchmark to use first-principles in obtaining elastic coefficients as a function of temperature.

Acknowledgements

This work is funded by the National Science Foundation (NSF) through grant DMR-0510180. First-principles calculations were carried out on the LION clusters supported by the Materials Simulation Center and the Research Computing and Cyber infrastructure unit at Pennsylvania State University. We would like to thank the members of the Phases Research Lab, at the Pennsylvania State University for their stimulating discussions.

References

[1] A. Kato, T. Yagi, N. Fukusako, J. Phys. Condens. Matter 21 (2009).
[2] R. Saravanan, M.C. Robert, J. Alloys Compd. 479 (2009) 26–31.
[3] M.J. Yang, L.M. Zhang, Q. Shen, J. Wuhan Univ. Technol.: Mater. Sci. Ed. 24 (2009) 912–916.
[4] C.H. Lee, S.H. Lee, S.Y. Chun, S.J. Lee, J. Nanosci. Nanotechnol. 6 (2006) 3429–3432.
[5] V.K. Zaitsev, M.I. Fedorov, E.A. Gurieva, I.S. Eremin, P.P. Konstantinov, A.Y. Samunin, M.V. Vedernikov, Phys. Rev. B 74 (2006) 045207.
[6] L. Chuang, N. Savvides, S. Li, J. Electron. Mater. 38 (2009) 1008–1012.
[7] G.A. Stringer, R.J. Higgins, J. Appl. Phys. 41 (1970) 489–497.
[8] Y.H. Duan, Y. Sun, J. Feng, M.J. Peng, Physica B 405 (2010) 701–704.
[9] O. Benhelal, A. Chahed, S. Laksari, B. Abbar, B. Bouhafs, H. Aourag, Phys. Status Solidi B 242 (2005) 2022–2032.
[10] J.L. Corkill, M.L. Cohen, Phys. Rev. B: Condens. Matter 48 (1993) 17138–17144.
[11] L. Xiunu Sophie, W. Dongli, M. Beekman, G. Nolas, Synthesis and Thermoelectric Properties of Antifluorite Materials, Materials Research Society, Warrandale, PA, USA, 2008, pp. 469–474.
[12] C.L. Zhang, P.D. Han, X. Yan, C. Wang, L.Q. Xia, B.S. Xu, J. Phys. D: Appl. Phys. 42 (2009) 125403.
[13] R.G. Schwartz, J. Solid State Chem. 3 (1971) 533–540.
[14] G.A. Roberts, E.J. Cairns, J.A. Reimer, J. Power Sources 110 (2002) 424–429.
[15] J.-I. Tani, M. Takahashi, H. Kido, J. Alloys Compd. 485 (2009) 764–768.
[16] H. Ledbetter, Handbook of Elastic Properties of Solids, Liquids, and Gases, vol. II, Academic, San Deigo, 2001, pp. 57–64.
[17] D.G. Pettifor, Mater. Sci. Technol. 8 (1992) 345–349.
[18] S.F. Pugh, Philos. Mag. 45 (1954) 823–843.
[19] M. Hebbache, Solid State Commun. 113 (2000) 427–432.
[20] D.M. Teter, MRS Bull. 23 (1998) 22–27.
[21] Z. Ding, S. Zhou, Y. Zhao, Phys. Rev. B 70 (2004) 184117.
[22] S. Ganeshan, S.L. Shang, H. Zhang, Y. Wang, M. Mantina, Z.K. Liu, Intermetallics 17 (2009) 313–318.
[23] J.X. Yi, P. Chen, D.L. Li, X.B. Xiao, W.B. Zhang, B.Y. Tang, Solid State Commun. 150 (2010) 49–53.
[24] M.B. Kanoun, S. Goumri-Said, A.H. Reshak, Comput. Mater. Sci. 47 (2009) 491–500.
[25] H. Ogi, T. Shagawa, N. Nakamura, M. Hirao, H. Odaka, N. Kihara, Phys. Rev. B 78 (2008) 134204.
[26] T.E. Karakasidis, C.A. Charitidis, Theor. Appl. Fract. Mech. 51 (2009) 195–201.
[27] H. Ledbetter, R.P. Reed, J. Phys. Chem. Ref. Data 2 (1974) 531–618.
[28] S.M. Foiles, Scripta Mater. 62 (2010) 231–234.
[29] Z.K. Liu, H. Zhang, S. Ganeshan, Y. Wang, S.N. Mathaudhu, Scripta Mater. (accepted) (2010), http://dx.doi.org/10.1016/j.scriptamat.2010.03.049.
[30] Y. Wang, J.J. Wang, H. Zhang, V.R. Manga, S.L. Shang, L.Q. Chen, Z.K. Liu, Acta Mater. (under review) (2009).
[31] H. Zhang, S.L. Shang, Y. Wang, A. Saengdeejing, L.Q. Chen, Z.K. Liu, Acta Mater. (under review) (2010).
[32] W. Kohn, L.J. Sham, Phys. Rev. 140 (1965) A1133–A1138.
[33] J.P. Perdew, K. Burke, M. Ernzerhof, Phys. Rev. Lett. 77 (1996) 3865–3868.
[34] G. Kresse, J. Furthmuller, Phys. Rev. B 54 (1996) 11169–11186.
[35] G. Kresse, J. Furthmuller, Comput. Mater. Sci 6 (1996) 15–50.
[36] G. Kresse, D. Joubert, Phys. Rev. B 59 (1999) 1758–1775.
[37] H.J. Monkhorst, J.D. Pack, Phys. Rev. B 13 (1976) 5188–5192.
[38] M. Methfessel, A.T. Paxton, Phys. Rev. B 40 (1989) 3616–3621.
[39] P.E. Blochl, O. Jepsen, O.K. Andersen, Phys. Rev. B 49 (1994) 16223–16233.
[40] S.L. Shang, Y. Wang, Z.K. Liu, Appl. Phys. Lett. 90 (2007) 101909.
[41] S. Ganeshan, S.L. Shang, Y. Wang, Z.K. Liu, Acta Mater. 57 (2009) 3876–3884.
[42] R. Hill, Proc. Phys. Soc. London 65 (1952) 396–1396.
[43] W. Voigt, Lehrbuck der Krystallphysik, B.G. Teubner, Leipzig, 1928.
[44] A. Reuss, ZAMM 9 (1929) 49–58.
[45] A. van de Walle, Calphad-Comput. Coupling Ph. Diagrams Thermochem. 33 (2009) 266–278.
[46] R. Arroyave, D. Shin, Z.K. Liu, Acta Mater. 53 (2005) 1809–1819.
[47] W.J. Golumbfskie, R. Arroyave, D. Shin, Z.K. Liu, Acta Mater. 54 (2006) 2291–2304.
[48] S.L. Shang, Y. Wang, H. Zhang, Z.K. Liu, Phys. Rev. B 76 (2007) 052301.
[49] A. van de Walle, G. Ceder, Rev. Mod. Phys. 74 (2002) 11.

[50] G.F. Davies, J. Phys. Chem. Solids 35 (1974) 1513–1520.
[51] N. Wakabaya, H.R. Shanks, A.A.Z. Ahmad, G.C. Danielso, Phys. Rev. B 5 (1972) 2103–2107.
[52] R.J. Kearney, T.G. Worlton, R.E. Schmunk, J. Phys. Chem. Solids 31 (1970) 1085–1097.
[53] B.C. Gerstein, P.L. Chung, G.C. Danielso, J. Phys. Chem. Solids 27 (1966) 1161–1165.
[54] B.C. Gerstein, F.J. Jelinek, M. Habensch, W.D. Shickell, J.R. Mullaly, P.L. Chung, J. Chem. Phys. 47 (1967) 2109–2115.
[55] F.J. Jelinek, W.D. Shickell, B.C. Gerstein, J. Phys. Chem. Solids 28 (1967) 267–270.
[56] Non-Tetrahedrally Bonded Elements and Binary Compounds I, in: Landolt Bornstein-Group III Condensed Matter, vol 41C, Springer-Verlag, 1998.
[57] W.B. Whitten, P.L. Chung, G.C. Danielson, J. Phys. Chem. Solids 26 (1965) 49–56.
[58] P.L. Chung, W.B. Whitten, G.C. Danielso, J. Phys. Chem. Solids 26 (1965) 1753–1760.
[59] L.C. Davis, W.B. Whitten, G.C. Danielson, J. Phys. Chem. Solids 28 (1967) 439–447.
[60] H. Ledbetter, Mater. Sci. Eng. A 442 (2006) 31–34.
[61] V. Tvergaard, J.W. Hutchinson, J. Am. Ceram. Soc. 71 (1988) 157–166.
[62] X. Luo, B. Wang, J. Appl. Phys. 104 (2008) 073518.
[63] H. Fu, W. Peng, T. Gao, Mater. Chem. Phys. 115 (2009) 789–794.
[64] M.H. Yoo, Scripta Metall. 20 (1986) 915–920.
[65] H.Z. Fu, D.H. Li, F. Peng, T. Gao, X.L. Cheng, Comput. Mater. Sci. 44 (2008) 774–778.
[66] W.A. Counts, M. Friák, D. Raabe, J. Neugebauer, Acta Mater. 57 (2009) 69–76.